Biogeosciences Discuss., 10, 4851–4886, 2013
www.biogeosciences-discuss.net/10/4851/2013/
doi:10.5194/bgd-10-4851-2013

Biogeosciences
Discussions
Open Access

Distribution of the Fukushima-derived radionuclides in seawater in the Pacific off the coast of Miyagi, Fukushima, and Ibaraki Prefectures, Japan

S. Oikawa, H. Takata, T. Watabe, J. Misonoo, and M. Kusakabe

Head Office, Marine Ecology Research Institute, Towa-Edogawabashi Building 7F,
347 Yamabuki-cho, Shinjuku, 162-0801 Tokyo, Japan

Received: 28 December 2012 – Accepted: 5 February 2013 – Published: 11 March 2013

Correspondence to: H. Takata (takata@kaiseiken.or.jp)

Published by Copernicus Publications on behalf of the European Geosciences Union.

Abstract

The activities of artificial radionuclides in seawater samples collected off the coast of Miyagi, Fukushima, and Ibaraki Prefectures were measured as part of a monitoring program initiated by the Japanese government Ministry of Education, Sports, Science and Technology immediately after the Fukushima Dai-ichi nuclear power plant accident. The spatial and temporal distributions of those activities are summarized herein. The activities of strontium-90, iodine-131, cesium-134 and -137 (i.e. ^{90}Sr, ^{131}I, ^{134}Cs, and ^{137}Cs) derived from the accident were detected in seawater samples taken from areas of the coastal ocean adjacent to the power plant. No ^{131}I was detected in surface waters (≤ 5 m depth) or in intermediate and bottom waters after 30 April 2011. Strontium-90 was found in surface waters collected from a few sampling stations in mid-August 2011 to mid-December 2011. Temporal changes of ^{90}Sr activity in surface waters were evident, although the ^{90}Sr activity at a given time varied widely between sampling stations. The activity of ^{90}Sr in surface waters decreased slowly over time, and by the end of December 2011 had reached background levels recorded before the accident. Radiocesium, ^{134}Cs and ^{137}Cs, was found in seawater samples immediately after the accident. There was a remarkable change in ^{137}Cs activities in surface waters during the first 7 months (March through September 2011) after the accident; the activity reached a maximum in the middle of April and thereafter decreased exponentially with time. Qualitatively, the distribution patterns in surface waters suggested that in early May ^{137}Cs-polluted water was advected northward; some of the water then detached and was transported to the south. Two cores of the water with high ^{137}Cs activity persisted at least until July 2011. In subsurface waters ^{137}Cs activity was first detected in the beginning of April 2011, and the water masses were characterized by σ_t (an indicator of density) values of 25.5–26.5. From 9–14 May to 5–16 December 2011, the depths of the water masses increased with time, an indication that deepening of the isopycnals with time can be an important mechanism for the transport of ^{137}Cs downward in coastal waters. During 4–21 February 2012, the water column became

vertically homogeneous, probably because of convective mixing during the winter, the result being nearly constant values of ^{137}Cs activity throughout the water column from the surface to the bottom (~ 200 m depth) at each station.

1 Introduction

At 05:46 UTC on 11 March 2011, the Great East Japan Earthquake and ensuing tsunami caused serious damage to the natural environment of Japan. At the Tokyo Electric Power Company's Fukushima Dai-ichi nuclear power plant (FDNPP), which consists of six boiling water reactor units, a series of very large tsunami waves damaged the electrical system, and the external power supply was lost because of the earthquake. Two emergency diesel electric generators then quickly started up, but all alternating current power supplies were lost after the two emergency diesel generators stopped as a result of damage caused by a series of tsunami waves.

At 06:36 UTC on the day following the accident, a hydrogen explosion occurred in the Unit 1 reactor building as a result of the failure of the cooling system for the nuclear reactor. On 14 March a hydrogen explosion also occurred in the Unit 3 reactor. Although the Unit 4 reactor had been shut down and the fuel rods transferred to the spent fuel pool, an explosion occurred in the Unit 4 reactor building on 15 March. On the same day, an explosion that occurred in the Unit 2 reactor caused a drop of pressure in the suppression pool at the bottom of the containment vessel. As a result of these explosions, a large amount of radioactive material was discharged into the environment. The Japanese Government estimated the amounts of ^{131}I, ^{134}Cs, and ^{137}Cs discharged into the atmosphere to be 160, 18, and 15 PBq, respectively, from 11 March to 5 April 2011 (Nuclear Emergency Response Headquarters, Government of Japan, NERH, 2011). Results of environmental monitoring suggested that ^{131}I and ^{137}Cs derived from the FDNPP were present within three days after the accident in atmospheric particles at Fukuoka Prefecture, western Japan, more than 1000 km from the FDNPP (Momoshima et al., 2012). In the meantime, a large amount of wastewater had accumulated at the sites of the Unit 1, 2, and 3 reactors because of the use of large volumes of cooling water to prevent the occurrence of a more serious nuclear accident. Although the total volume of highly contaminated wastewater is unknown, the water that accumulated in the reactor buildings leaked out through underground conduits into the ocean. From numerical simulations, Tsumune et al. (2012) estimated that the direct release of radioactively contaminated liquid wastes into the ocean started on 26 March 2011 and that the total amount of ^{137}Cs in the liquid wastes was 3.5 ± 0.7 PBq.

About ten days after the accident, the Marine Ecology Research Institute started an environmental radioactivity monitoring program, with a particular focus on the offshore ocean, by taking seawater samples and performing analyses of radioactivity. In response to changes in societal concerns, the monitored area of the ocean has expanded progressively since that time. The radioactivity data obtained during the monitoring program have been published on the MEXT website (http://radioactivity.mext.go.jp/en/list/259/list-1.html). In this paper, we compile and revise, if necessary, the data on ^{90}Sr, ^{131}I, ^{134}Cs, and ^{137}Cs activities in seawater samples collected outside the area in 30 km radius of the plant off the coast of Miyagi, Fukushima, and Ibaraki Prefectures immediately after the FDNPP accident. We furthermore describe the spatiotemporal variations of the ^{134}Cs and ^{137}Cs activities in seawater samples collected every two months from the coastal ocean east of Japan during the time immediately after the accident until the end of February 2012. We investigated the mechanisms that control the distribution of ^{137}Cs in the water column from the surface to the bottom by using a suite of complementary measurements of other parameters, which are not available on the MEXT website, including salinity, temperature, and σ_t, an indicator of density of a given temperature. Thus, we can evaluate the influence of oceanic processes on radionuclide behavior in the coastal waters using the parameters.

Activities of ^{137}Cs in surface seawaters after the accident have been reported (Aoyama et al., 2012; Buesseler et al., 2012; Honda et al., 2012). These reports indicate that the ^{137}Cs that originated from the FDNPP migrated as far as ∼ 600 km from the shore because of nearshore eddies and the Kuroshio Current. With respect to subsurface waters, the vertical distributions of ^{137}Cs have been reported, and ^{137}Cs activities that were relatively high compared to those in the waters before the accident (MEXT, 2010) have been observed (Buesseler et al., 2012). However, the vertical transport mechanisms for radiocesium in the area are not fully understood. In general, two main processes are thought to transport ^{137}Cs downward: (1) sinking particles and (2) vertical turbulent mixing (e.g., diapycnal and isopycnal mixing). Before the FDNPP accident, the main source of ^{137}Cs in seawater in the North Pacific had been fallout from past nuclear weapons tests and the Chernobyl accident. In those cases, ^{137}Cs was deposited onto the sea surface from the atmosphere and then transported downward by sinking particles (Fowler et al., 1987; Kusakabe et al., 1988). Also, ^{134}Cs and ^{137}Cs that originated from the Chernobyl accident were detected in sediment traps deployed at depths of 110–780 m in the North Pacific and Bering Sea within a few months after the accident (Kusakabe et al., 1988). In case of the FDNPP accident, however, direct discharge of wastewater is a main source for the coastal seawaters where physical processes, such as coastal currents and vertical mixing driven by diurnal tidal currents, are also thought to transport radiocesium downward in seawaters off the coast of Miyagi, Fukushima, and Ibaraki Prefectures. As for vertical turbulent mixing, diapycnal mixing in these coastal areas is mainly affected by diurnal tidal currents during the spring and autumn. It has been reported that the vertically homogeneous physical structure of the water column (i.e., σ_t, salinity, and temperature) results from vigorous vertical mixing of the water column during periods of strong tidal currents (e.g., Matsuura et al., 2007). During the winter, the vertical distributions of temperature, salinity, σ_t, and other properties (e.g., nutrient concentrations) indicate that the surface waters are homogeneous, unstable, and presumably well mixed to depths ranging from one to several hundred meters. In addition, isopycnal mixing at the σ_t of the thermostad could contribute to the transport of radiocesium from the surface to the middle and bottom of the water column. If the isopycnal surfaces deepen, for example, radiocesium can be transported downward. Thus, discussion of these two processes is a key to a better understanding of radiocesium behavior in the coastal seawaters off Miyagi, Fukushima, and Ibaraki Prefectures.

2 Materials and methods

2.1 Survey areas and sampling

The survey areas are shown in Fig. 1. Seawater samples were collected from the surface (≤ 5 m depth) to near the bottom (~ 30 m above the seafloor) at each sampling station (Table 1). Sampling cruises are listed in Table 1 in the Supplement. To elucidate trends in the distribution of radionuclides during the survey (from the middle of March 2011 to the middle of February 2012), the locations of sampling stations were changed from 30 km offshore from the FDNPP to oceanic locations further offshore. Thus, the sampling period of 1 year was divided into two phases as follows.

2.1.1 Phase 1 (23 March 2011 to 7 May 2011)

On 23 March 2011 we began the first survey (Fig. 1b). Phase 1 involved four cruises: KH11-E01, MR11-E01, KR11-E02, and YK11-E02. Because the focus of this phase was on detection of radioactivity from the FDNPP, we chose eight sampling stations (1-1 to 1-4 and 2-1 to 2-4) located in the western North Pacific Ocean 30 km off the coast from the FDNPP. In the middle of the survey period, we added several more stations (i.e. 2-5, 2-6, S1, S2, S3 and S4) so that the stations formed a U-shape surrounding the FDNPP. We used a Niskin type water sampler with a CTD system (SBE 9 plus, Sea-Bird Electronics, Inc., Bellevue, WA, USA) to collect water samples. Because of the urgent nature of the survey, only a few liters of seawater was collected at each station. The samples were returned to a laboratory without addition of any acids. This urgent survey lasted two months after the accident.

2.1.2 Phase 2 (9 May 2011 to the end of February 2012)

On 9 May 2011, we began the second survey, which involved an expanded sampling area in the western North Pacific Ocean (Fig. 1c). Seawater samples were taken from 2, 3, or 4 depths, namely the surface (≤ 5 m depth), and intermediate and bottom depths. During the phase, we used a Van Dorn type water sampler with a CTD system (SBE 19, Sea-Bird Electronics, Inc., Bellevue, WA, USA) to collect water samples. Although it would be difficult to define ”bottom water” precisely from a physical oceanographic standpoint, bottom water in this study meant water that was obtained for reasons of convenience ≤ 30 m above the seabed. Similarly, the term “intermediate water” was used to characterize water that was obtained at depths of 10 m (Stn. J1), 50 m, 100 m, and 200 m and in some cases was the deepest water sample collected at a station.

2.2 Radioactivity measurements

2.2.1 ^{131}I, ^{134}Cs, and ^{137}Cs measurements

During Phase 1, we used a coaxal type high purity Ge detector (i.e. ORTEC GAMMA-X detectors (series GMX40), relative efficiency: 44%, SEIKO EG&G Co. LTD) to measure radioactivity by gamma-ray spectrometry for several tens of minutes in a 0.5–2 L sample of seawater in a Marinelli container. The detection limits of ^{131}I, ^{134}Cs, and ^{137}Cs were roughly calculated to be 11, 10, and 10 Bq L^{-1}, respectively, based on measurements of the corresponding gamma-ray photopeaks at 364.5, 604.7, and 661 keV. However, activities below the detection limit were also evaluated by counting for a extended time because of the emergency nature of the circumstances. As for some curises during Phase 2 (i.e. NT11-E01, MR11-E02, YK11-E05R, and KR11-E04R), a 2 L sample of seawater was measured by the same method.

For most of the water samples collected during Phase 2, a volume of 2 L or 40–60 L was used for the radiocesium analyses, with chemical separation achieved by co-precipitation after the addition of a Cs^+ carrier. The pH of the seawater sample was adjusted to nearly 1 with hydrochloric acid when cesium was co-precipitated with ammonium phosphomolybdate (AMP: KISHIDA Chemical Co., LTD). The recovery of Cs with AMP turned out to be about 100 %. The activity of radiocesium (^{134}Cs and ^{137}Cs) co-precipitated with AMP was measured with coaxial type Ge detectors (Canberra GC40 series, relative efficiency: 40 %, and Eurisys EGPC series, relative efficiency: 89%, Canberra Japan KK) for a few hours. Inoue et al. (2012) have pointed out that the cascade summing effect should not be disregarded for the 604.7 and 795.8 keV photopeaks emitted from ^{134}Cs when measurements are carried out with the sample close to the Ge detector. In our measurements, we avoided this error for all of the seawater samples by using computer software to correct for the contribution of the cascade summing of ^{134}Cs with the peak/total ratio method. When the detection limit of the ^{134}Cs and ^{137}Cs radioactivity was chosen to be three times the noise level of the counting, the minimum detectable activities of ^{134}Cs and ^{137}Cs were expected to be 0.1–1.0 mBq L^{-1} for counting times of tens of thousands of seconds. The radioactivities of ^{134}Cs and ^{137}Cs in the water samples were decay-corrected to the sampling date.

2.2.2 ^{90}Sr measurements

In order to measure the ^{90}Sr in water samples, we used the same water samples that were used for radiocesium measurements. The supernatant from which the AMP had been removed was passed through a cation exchange resin column (Dowex 50W-X8, 100–200 mesh, 9 cmφ ×32 cm) to remove Mg, an element present in seawater that would interfere with the analysis. After the addition of sodium carbonate, the pH of the seawater sample was raised with a solution of sodium hydroxide to co-precipitate Sr together with carbonate precipitates. The precipitates thus formed were boiled for approximately 2 h before being allowed to settle overnight. The sample supernatant was then carefully removed and discarded, and the carbonate precipitate was separated from solution by centrifugation. The precipitate was dissolved in hydrochloric acid and evaporated to dryness. The residue was dissolved in dilute hydrochloric acid and passed through a cation exchange resin column (Dowex 50W-X8, 100–200 mesh, 3 cmφ × 26 cm) for the complete removal of Ca. The activity of ^{90}Sr was determined by using a gas-flow type low background anti-coincidence beta counter (e.g., LBC-471Q, Aloka Co. Ltd., Japan) to count the beta rays emitted from ^{90}Y at radio-equilibrium with ^{90}Sr. The detection limit of ^{90}Sr radioactivity, taken as sum of measurement result and three times of its counting statistics error, was about 0.4 mBq L^{-1} with 100 min counting for a 50 L of seawater sample.

3 Results and discussion

3.1 Activities of ^{131}I, ^{134}Cs, and ^{137}Cs in seawater (Phase 1)

On 23 March 2011, the presence of ^{131}I, ^{134}Cs, and ^{137}Cs was first confirmed in the surface waters (≤ 5 m depth) collected at sampling stations during the first cruise (KH11-E01) from 23–27 March. The ^{131}I, ^{134}Cs, and ^{137}Cs activities that we detected are summarized in Table 2 together with the ^{131}I/^{137}Cs and ^{134}Cs/^{137}Cs activity ratios. The activities found in the surface waters fell in the ranges 24.9–76.8, 11.2–21.4, and 11.2–26.1 Bq L^{-1} for ^{131}I, ^{134}Cs, and ^{137}Cs, respectively. The activity of ^{131}I at each sampling station varied considerably.

Temporal changes of ^{131}I activity and ^{131}I/^{137}Cs activity ratios in the surface waters are shown in Fig. 2. Activities of ^{131}I in surface water decreased rapidly until the end of March 2011, increased abruptly in the middle of April, and then decreased again until the end of April 2011 (Fig. 2a), a pattern reflecting the direct discharge of polluted waters from the FDNPP. In addition, the ^{131}I/^{137}Cs activity ratio fluctuated appreciably until the beginning of April 2011 and then decreased with an estimated half-life of 6.4 days, which is shorter than the physical half-life of ^{131}I (8.02 days). This result reflects the advection of contaminated waters by coastal and/or ocean currents. After the end of April 2011, no ^{131}I was found in the surface, intermediate, or bottom waters (Fig. 2b).

We have been monitoring the ^{137}Cs activity in surface waters at fixed 8 points (37°00–40′ N, 141°19–25′ E) that are approximately 6 km east of the sampling stations in Fig. 1b for 28 years as part of a nationwide surveillance project before the accident (Oikawa et al., 2013). According to the monitoring results, ^{137}Cs activities in surface waters during the five years preceding the accident (2006–2010) had apparently reached a nearly constant level of 1.6 ± 0.26 mBq L^{-1}, the range of activities being 1.1–2.2 mBq L^{-1}. In this study, the maximum ^{137}Cs activity during the first cruise (KH11-E01), 26 Bq L^{-1} at Stn. 1-3 on 24 March, was 16 250 times the average value during the preceding five years. The radioactive materials released into the atmosphere from the FDNPP would have been swept upwards by air currents and transported horizontally by the prevailing winds. It is unclear to what extent the transport pathways of the ^{131}I, ^{134}Cs, and ^{137}Cs found in the surface waters involved ultramicroscopic solid particles or liquid droplets dispersed or suspended in the air or seawater. The ^{131}I/^{137}Cs activity ratio in the water samples ranged from 0.28 to 11 (Fig. 2b). In addition, the ^{131}I/^{137}Cs activity ratio increased during the period at all stations except Stn. 1-1. In contrast, the ^{134}Cs/^{137}Cs activity ratio in the surface waters after the direct discharge was apparently constant at 0.93 (Table 2), a value higher than the corresponding ratio of 0.5 in the Chernobyl fallout (UNSCEAR, 2000).

Beginning on 28 March 2011 (cruise: MR11-E01 (3/28–4/9), KR11-E02 (4/11–4/21), and YK11-E02 (4/25–5/7)), we collected water from both intermediate and bottom depths in addition to the surface water monitoring to clarify the vertical dispersion or advection of the radionuclides. The ^{131}I, ^{134}Cs, and ^{137}Cs activities in the intermediate and bottom water samples are listed in Table 3 together with the ^{131}I/^{137}Cs and ^{134}Cs/^{137}Cs activity ratios. As expected, we detected ^{131}I, ^{134}Cs, and ^{137}Cs in intermediate and bottom waters in addition to surface waters during the MR11-E01 cruise (3/28–4/9). However, the ^{131}I/^{134}Cs and ^{131}I/^{137}Cs ratios were scattered in intermediate and bottom waters (Table 2). This scatter may reflect complexity in sources of atmosphere and direct discharge because both sources are thought to have different activity ratios of ^{131}I/^{134}Cs and ^{131}I/^{137}Cs (Fig. 2b).

3.2 Spatial and temporal distributions of radiocesium in seawater (Phase 2)

During the middle of the Phase 1 survey, the ^{134}Cs/^{137}Cs activity ratio was nearly constant at 0.93, the indication being that both ^{134}Cs and ^{137}Cs were mainly derived from the FDNPP accident. We therefore focused on the ^{137}Cs data to elucidate the spatial and temporal distribution of radiocesium during the roughly one-year duration of the Phase 2 survey because the half-life of ^{137}Cs is relatively long (about 30 years) compared to that of ^{134}Cs (about 2 years).

Figure 3 shows the temporal variation of ^{137}Cs activities obtained at all the monitoring stations for about one year after the accident. The observed ^{137}Cs activity was a maximum (186 Bq/L) in surface waters (≤ 5 m depth) at Stn. 1-4 on 15 April 2011 during Phase 1 and then declined exponentially during the following three months from May to July 2011. From August 2011 to February 2012, the activity of ^{137}Cs in the surface waters decreased slightly. About one month after direct release of contaminated wastewaters from the FDNPP reactors (26 April 2011: Tsumune et al., 2012), activities of ^{137}Cs in subsurface waters near the FDNPP (30 km distance) were clearly higher than the background activities (1.3–2.0 mBq L^{-1}) in coastal seawater of the western North Pacific prior to the accident (Inomata et al., 2009; MEXT, 2010; Oikawa et al., 2011). Moreover, even at the stations located far from the FDNPP (e.g., Stns. A1, B1, G1, and I1: see Fig. 1c), ^{137}Cs activities were high in subsurface waters (i.e., intermediate and bottom waters) on May 2011 (cruises 11WM01 and 11WM02: see Table 1 in Supplement). These results indicate that radiocesium derived from the FDNPP was dispersed laterally and vertically during a period of 2–3 months.

To better understand the distribution of radiocesium throughout the water column in the coastal sea off Miyagi, Fukushima, and Ibaraki Prefectures, it was necessary to investigate oceanic processes such as the advection of water masses, vertical mixing in the water column, and scavenging by particles. Thus, in the following section we use data obtained during the ten cruises (11WM01 (9–14 May 2011) to 11WM14

(4–21 February 2012), Table 1 in Supplement) to discuss spatial and temporal changes in the distribution of ^{137}Cs in the coastal ocean.

3.2.1 Temporal changes in distribution of ^{137}Cs in surface seawaters

Figure 4 shows the temporal changes in the distributions of temperature, salinity, and ^{137}Cs activities in surface waters from 9–14 May 2011 to 4–21 February 2012. During 9–14 May, high ^{137}Cs activities (~1.0 Bq L^{-1}) were observed in northern and northeastern areas (from Stns. B1-3 to E1-3; see Fig. 1C). In contrast, the ^{137}Cs activities at stations located to the southeast of the FDNPP were relatively low. Specifically, they were 0.14, 0.035, and 0.61 Bq L^{-1} at Stns. F1, G2, and H1, respectively. However, the ^{137}Cs activity at Stn. G1 was high (5.4 Bq L^{-1}). This variability reflects the complexity of coastal currents. Tsumune et al. (2012) have argued that a water mass with high ^{137}Cs activity had been transported southward along the coast by the coastal current until April, and that the water mass was then advected northward during May, the result being a northward dispersion of ^{137}Cs following the initial southward dispersion.

At stations I1–3 to L1–4 located to the south and far from the FDNPP (Fig. 1C), ^{137}Cs activities during 9–14 May 2011 ranged between 2.5 mBq L^{-1} and 0.11 Bq L^{-1} or were below the limit of detection (Fig. 4). The low ^{137}Cs values are thought to have resulted from the presence of a cyclonic mesoscale eddy, which was present by the end of May (Kawamura et al., 2011; Tsumune et al., 2012). The presence of the eddy was also evidenced by high temperatures (~ 20 °C) and high salinities (> 34) in the corresponding area. The eddy disappeared during the period 6–10 June. Simultaneously, ^{137}Cs activity at Stns. J1–3 to L1–2 increased. In particular, relatively high activities (1.0–4.6 Bq L^{-1}) were observed at Stns. I1, J1, K1, and L1 near the coastline.

At Stns. A1–3 to the north and far from the FDNPP (Fig. 1), ^{137}Cs activities in surface waters were higher than background values. However, the ^{137}Cs activities were lower in these surface waters from 9–14 May to 6–10 June than in surface waters at Stns. B1–4, which are closer to the FDNPP. The resulting pattern was similar to that observed in the southern area (Stns. I-series to L-series): the water mass at Stns. A1–3 (salinity: > 34) was different from that at Stns. B1–4 (salinity: >33), as depicted in Fig. 4. It is thought that transport of ^{137}Cs further north was inhibited by the presence of the high-salinity water mass and/or that ^{137}Cs activities were diluted by intrusion of a water mass with low ^{137}Cs activities. The ^{137}Cs activities gradually decreased from 6–10 June 2011 to 4–21 February 2012.

3.2.2 Temporal changes in the distribution of ^{137}Cs in intermediate and bottom waters

The activities of ^{137}Cs at depths >5 m for all the stations ranged from 2.0 mBq L^{-1} to 11 Bq L^{-1} with a geometric mean of 47 mBq L^{-1} during the period 4–14 May 2011. During 23–27 May 2011, the mean values to 57 mBq L^{-1} and then reached a maximum of 95 mBq L^{-1} on 6–10 June 2011. These results suggest that waters containing high activities of ^{137}Cs derived from the FDNPP were transported downward by dynamic mixing and/or diffusion during the sampling periods.

A plot of ^{137}Cs activities for each sampling depth versus time (Fig. 5) reveals that at Stns. D1, E1, F1, and G1 (near the FDNPP) ^{137}Cs activities at a depth of 50 m increased by factors of 3–10 in about 1 month (from 9–14 May 2011 to 6–10 June 2011), the maxima being 0.39, 0.21, 0.36, and 0.21 Bq L^{-1} at Stns. D1, E1, F1, and G1, respectively. Similar results were obtained even at Stns. D3, E3, F3, and G3, which were located about 100 km further from the coast than Stns. D1–G1. In addition, at a depth of 100 m, the maximum activity was measured at Stn. E3 (56 mBq L^{-1}) on 7 June 2011 or about two weeks later at Stns. D3 (72 mBq L^{-1}), F3 (0.18 Bq L^{-1}), G3 (0.1 Bq L^{-1}), and H3 (0.1 Bq L^{-1}). The ranges of ^{137}Cs activities at 50 and 100 m at these stations are comparable to those in the surface waters during June 2011 (Fig. 5). From 7–15 September 2011 to 4–21 February 2012, the ranges of ^{137}Cs activities in the bottom waters were similar to the ranges in the surface waters at all the stations, with the exception of Stns. A3 and J3. The activities of ^{137}Cs in the bottom waters at these stations on 7–15 September 2011 were clearly higher than before the accident (MEXT, 2010). At those two exceptional stations, ^{137}Cs activities in the bottom waters

(453–576 m depth) ranged between 0.78 and 1.7 mBq L^{-1} throughout the sampling periods. Moreover, the fact that ^{134}Cs was not detected in the bottom waters at Stns. A3 and J3 suggests that ^{137}Cs derived from the FDNPP was not transported to such relatively great depths. The implication is that ^{137}Cs was transported to depths as great as ~200 m in coastal waters within six months after the FDNPP accident.

Two main processes are thought to transport ^{137}Cs downward. One is release of ^{137}Cs back into the water column from sinking particles, and the other is vertical mixing of water. In general, sinking particles include biogenic and lithogenic materials. Zooplankton excretion is considered to account for the vertical transport of sinking biogenic particles, the production of fecal pellets acting as a biological pump (Honda et al., 2002). On the basis of sediment trap data and plankton collections, Fowler et al. (1987) previously reported that radioisotopes from the Chernobyl accident were removed from surface waters of the Mediterranean Sea by zooplankton grazing, the consumed radionuclides having been packaged into large fecal pellets that sank rapidly.

In the coastal waters off Fukushima and Miyagi Prefectures, Kaeriyama et al. (2012) reported that ^{137}Cs activities in zooplankton at 50 m depth ranged from 0.88 to 29 Bq kg^{-1}-wet weight during June 2011 to February 2012, whereas ^{137}Cs activities in surrounding waters at the same depth were low (10 m Bq L^{-1} to 0.9 Bq L^{-1}). They estimated the zooplankton-to-water activity ratio of ^{137}Cs to be (3.3–4.4) ×10^{2} L/kg. These ratios are clearly higher than the reported concentration ratio of Cs for zooplankton (10 L/kg) published by the IAEA (2004). However, the contribution of zooplankton to the downward flux of ^{137}Cs through the subsurface water column within a few months after the FDNPP accident is thought to be small because the biomass of zooplankton is not high. For example, Kaeriyama et al. (2008) showed that the integrated biomass of zooplankton in the depth interval 0–150 m in coastal waters off Aomori and Iwate Prefectures (next to Miyagi Prefecture) ranged from 6.3 to 56.8 g-wet weight/m^{2} in October 2005 and June 2006. By multiplying this biomass by the ^{137}Cs activities in the zooplankton, we roughly estimated the inventory of Fukushima-derived ^{137}Cs in the zooplankton to be 5.5 m Bq m^{-2} to 1.6 Bq m^{-2} in the coastal areas. This range of

Title Page
Abstract | Introduction
Conclusions | References
Tables | Figures
◂◂ | ▸▸
◂ | ▸
Back | Close
Full Screen / Esc
Printer-friendly Version
Interactive Discussion

activities is considerably lower than the inventory of ^{137}Cs activity in coastal and open ocean waters (6.2–16 k Bq m^{-2} (Buesseler et al., 2012)).

Clay minerals derived from lithogenic materials are also known to accumulate ^{137}Cs (Comans et al., 1991; Sakuma and Kawamura, 2011; Kusakabe et al., 2013). In ^{137}Cs speciation experiments conducted by Otosaka and Kobayashi (2012), more than 75% of ^{137}Cs derived from the FDNPP in coastal sediments was adsorbed/incorporated onto/into irreversible fractions. Because we analyzed unfiltered seawater samples in this study, the samples would have included soluble, colloidal, and particulate fractions. The fraction of Cs associated with particles in water samples is expected to be small because Cs is not very particle-reactive (e.g., its distribution coefficient (K_d) = 4×10^3 L kg^{-1}) compared to other scavenging metals such as Mn, Fe, and Th (K_d: 2 $\times 10^6$ to 3×10^8 L kg^{-1} (IAEA, 2004; Takata et al., 2010)). Soluble forms are therefore expected to account for most of the ^{137}Cs activity in seawater samples, indicating the loss of relatively low amount of ^{137}Cs activities in waters by sinking of the radiocesium in particulate phase or the protection of ^{137}Cs in dissolved phase from scavenging because of its thermodynamically stable forms. It is thus unlikely that redistribution of ^{137}Cs in the water column into particles had much to do with the rapid increase of the ^{137}Cs activity in seawater at depths of 6–200 m.

Vertical water mixing can account for much of the downward flux of ^{137}Cs. There are two types of water mixing, diapycnal and isopycnal. Diapycnal mixing in coastal areas is mainly a function of diurnal tidal currents, the result being a vertically homogeneous structure of physical characteristics (i.e., σ_t, salinity, and temperature) of the water. In addition, during the winter, strong cooling and wind forcing of the mixed layer induce convection cells that extend to depths ranging from one to a few hundred meters. Figure 6 shows the temporal changes of σ_t in the coastal waters from 9–14 May 2011 to 4–21 February 2012. The formation of a vertically homogeneous water column during 4–21 February 2012 could be due to vigorous vertical mixing during the winter. This vertical mixing contributed to the downward flux of ^{137}Cs into bottom waters, the result being nearly constant ^{137}Cs activities throughout the water column at each station during

February 2012 (Fig. 5). However, ^{137}Cs derived from the FDNPP was observed at depths of ~ 200 m before the winter season (Fig. 5). Indeed, processes other than diapycnal mixing during the winter could have affected the vertical flux of ^{137}Cs in coastal waters during the period from 9–14 May to 5–16 December 2011.

Isopycnal mixing at the σ_t of the thermostad could contribute to the transport of ^{137}Cs from surface waters to intermediate and bottom waters. For example, chemical constituents such as the soluble forms of nutrients are transported or supplied along isopycnal surfaces (Sakai and Hiroe, 2002). From spring to autumn, diapycnal mixing attributed to the combined effects of coastal currents and diurnal tidal currents is thought to account for most vertical transport. In this study, however, a homogeneous water column was not observed at each station from 9–14 May to 5–16 December 2011 (Fig. 6), the differences in σ_t at each depth indicating that little diapycnal mixing was occurring.

The σ_t values in the coastal waters at all the stations near the FDNPP from 27 March 2011 to 7 May 2011 were in the range 25.5–26.5 (mean value: 26.1 ± 0.2) during the Phase 1 survey. Isopycnal lines reached bottom depths at Stns. A1–I1, B3, C3, and I3 or depths of about 200 m at Stns. A3 and D3–H3 by 5–16 December 2011 (Fig. 6). This result indicates that isopycnal surfaces at depths of ≤ 5 m became gradually deeper with time. To investigate the behavior of ^{137}Cs along isopycnal surfaces during the eight-month sampling period (from 9–14 May to 5–16 December 2011), we plotted in Fig. 7 the ^{137}Cs activities against σ_t at Stns. D1–G1 and D3–G3, the locations of which correspond to stations near the FDNPP during the Phase 1 survey (Fig. 1B). Most of the waters at 50 m, 100 m, and bottom depths from 9–14 May to 5–16 December 2011 were found to be within the σ_t range 25.5–26.5, and ^{137}Cs activities decreased in the order 50 m > 100 m (or bottom depth for Stn. D1) > bottom depth. There were some exceptions for Stns. D3 (50 and 100 m depths during 26–31 July) and E3 (100 m depth during 5–16 December), where ^{137}Cs activities were relatively low (Fig. 6); this result is probably attributable to the intrusion or mixing of water masses with low σ_t (Fig. 6) and low ^{137}Cs activities. At Stn. D3, the σ_t of the water column at depths of 50–100 m during 26–31 July was different from the σ_t during the time interval from 9–14 May to 5–9 July because of the presence of a water mass with low σ_t in the upper 100 m of the water column. This water mass was present in the upper 50 m of the water column before 26–31 July (Fig. 6). A similar trend was observed at a depth of 100 m at Stn. E3 during 5–16 December 2011. On the basis of these results, we concluded that during Phase 1 some of the ^{137}Cs-contaminated wastewater with σ_t values of 25.5–26.5 was diluted along isopycnal surfaces, and the depth of the surfaces became greater with time and reached about 200 m by 5–16 December. Thus, deepening of isopycnals with time can play an important role in the downward flux of ^{137}Cs in coastal waters during the spring-to-autumn time interval.

3.3 Temporal changes of ^{90}Sr in the surface water

Based on the results of the ^{134}Cs and ^{137}Cs radioactivity analyses, we conducted a strontium-90 survey with a limited number of water samples, the results of which are summarized in Table 4, together with activities of ^{90}Sr, ^{134}Cs, and ^{137}Cs and ^{90}Sr/^{137}Cs activity ratios. Activities of ^{90}Sr ranged from 1.2 to 4.3 mBq L^{-1}. The maximum activity of 4.3 mBq L^{-1} was observed at Stn. K1 on 14 October 2011 during the 11WM12 cruise and is about four times the usual background activity (approximately 1.6 mBq L^{-1} of the value in recent 5 yr (2006–2010; MEXT, 2010, 2011; Oikawa et al., 2013). In addition to the atmospheric releases, the cooling of the reactors with fresh water and seawaters, and the release of highly contaminated waste waters from the damaged reactor resulted in the direct discharges of radionuclides such as ^{90}Sr, ^{134}Cs and ^{137}Cs into the Pacific Ocean (Tsumune et al., 2011). During Augsut to November, the activities of ^{90}Sr in seawaters off Miyagi, Fukushima and Ibaraki were relatively high (0.22–0.43 mBq L^{-1}), suggesting that the FDNPP derived ^{90}Sr via direct discharge of waste waters was spread widely by coastal currents. Temporal changes in the activity of ^{90}Sr in surface waters are shown in Fig. 8. The activity of ^{90}Sr in surface waters decreased slowly over time and at a given time varied widely between sampling stations. By the end of 2011, the activity of ^{90}Sr in surface waters had reached the background levels recorded before the FDNPP accident.

Povinec et al. (2012) reported that ^{89}Sr (an indicator of treated water discharged from the FDNPP) and ^{90}Sr activities in surface water at a site near the FDNPP increased markedly on 5 December 2011 to 140 and 400 Bq L^{-1}, respectively, as a result of the release on 4 December 2011 of treated water that contained a considerable amount of radiostrontium. The water had been stored in a tank after removal of radiocesium by absorbers. In our study, however, an increase of radiostrontium activity, which would have provided convincing evidence for the release of radiostrontium from the FDNPP, was not observed from December 2011 to February 2012. The absence of such evidence was probably due to the fact that the sampling stations where water samples were analyzed for ^{90}Sr measurements were located far from the site of the FDNPP (Fig. 1c). Furthermore, during the winter vertical mixing is a major process (Fig. 6) that transports materials downward, not horizontally. It is likely that the high radiostrontium activity in the treated water was diluted by vertical mixing. Thus, while relatively high ^{90}Sr activities after the discharge was not observed activity ratio of ^{90}Sr/^{137}Cs increased by an order of magnitude in early December (Fig. 8b), in consistence with the timing of the second direct waste water discharge on 4 December. The Sr/Cs activity ratio can become a fingerprint to identify the pathways of Sr and Cs. This result would suggest that the treated water with high ratios of activity of ^{90}Sr to that of ^{137}Cs (Povinec et al., 2012) was transported to stations far from the FDNPP, while increased ^{90}Sr activities were not observed.

4 Conclusions

As a result of the FDNPP accident, large amounts of artificial radionuclides were uncontrollably released, mainly into the western North Pacific Ocean, because of atmospheric fallout and direct wastewater releases. During the time immediately after the accident, no one other than the TEPCO personnel could approach the waters within a

30-km radius of the FDNPP, the coastal waters being highly contaminated by radioactive materials.

Artificial radionuclides such as ^{131}I, ^{134}Cs, and ^{137}Cs derived from the FDNPP accident appeared consecutively in surface (≤ 5 m), intermediate, and bottom waters. However, ^{131}I in the surface waters decreased abruptly, and no ^{131}I was observed after the end of April 2011.

There was a remarkable change in ^{137}Cs activities in surface waters during the first 7 months (March–September 2011) of the monitoring. The distribution patterns in the surface waters suggest that in early May ^{137}Cs-polluted water was transported to the north, and then some of the water detached and was advected to the south. Two cores of the waters with high ^{137}Cs activity persisted at least until July. We believe that these results reflect the influence of coastal currents and the presence of an eddy. We observed relatively high ^{137}Cs activities derived from the FDNPP accident in subsurface waters. From 9–14 May to 5–16 December 2011, the depth of σ_t isopycnals of 25.5–26.5, initially ≤ 5 m, increased with time, an indication that deepening of water masses with time can be an important mechanism for transporting ^{137}Cs downward in coastal waters. During 4–21 February 2012, we observed the formation of a vertically homogeneous water mass, probably a consequence of vertical mixing processes during the winter, the result being nearly constant activities of ^{137}Cs throughout the water column from the surface to bottom (~ 200 m) at each station.

Fukushima-derived ^{90}Sr was found in surface waters collected at sampling stations from mid-August 2011 to mid-December 2011. The activities of ^{90}Sr at a given time varied widely between sampling stations. The activities of ^{90}Sr in the surface waters decreased slowly over time and by the end of December 2011 had reached the background level recorded before the FDNPP accident.

Supplementary material related to this article is available online at: http://www.biogeosciences-discuss.net/10/4851/2013/ bgd-10-4851-2013-supplement..pdf.

Acknowledgements. We thank Katsutoshi Kido and Kiriko Miyamoto for helpful discussions, and Sachiko Kiuchi for technical assistance. We also thank the captains and crews of research vessels of the JAMSTEC and Nippon Kaiyo Co. Ltd. for their help in the sampling. The marine environmental radioactivity survey is part of a research project contracted from the Japanese government Ministry of Education, Culture, Sports, Science and Technology.

References

Aoyama, M., Tsumune, D., Uematsu, M., Kondo, F., and Hamajima, Y.: Temporal variation of ^{134}Cs and ^{137}Cs activities in surface water at stations along the coastline near the Fukushima Dai-ichi Nuclear Power Plant accident site, Japan, Geochem. J., 46, 321–325, 2012.

Buesseler K. O., Jayne, S. R., Fisher, N. S., Rypina, I. I., Baumann, H., Baumann, Z., Breier, C. F., Douglass, E. M., George, J., Macdonald, A. M., Miyamoto, H., Nishikawa, J., Pike, S. M., and Yoshida, S.: Fukushima-derived radionuclides in the ocean and biota off Japan, PNAS 109, 5984–5988, 2012.

Comans, R. N. J., Haller, M., and DePreter, P.: Sorption of cesium on illite: non-equilibrium behavior and reversibility, Geochim. Cosmochim. Acta, 55, 433–440, 1991.

Fowler, S.,W., Buat-Menard, P., Yokoyama, Y., Ballestra, S., Holm, E., and Nguyen, H.,V.: Rapid removal of Chernobyl fallout from Mediterranean surface waters by biological activity, Nature 329, 56–58, 1987.

Honda, M.C., Imai, K., Nojiri, Y., Hoshi, F., Sugawara, T., and Kusakabe, M.: The biological pump in the northwestern North Pacific based on fluxes and major components of particulate matter obtained by sediment-trap experiments (1997–2000), Deep-Sea Res. Pt. II 49, 5595–5625, 2002.

Honda, M. C., Aono, T., Aoyama, M., Hamajima, Y., Kawakami, H., Kitamura, M., Masumoto, Y., Miyazawa, Y., Takigawa, M., and Saino, T.: Dispersion of artificial caesium-134 and -137 in the western North Pacific one month after the Fukushima accident, Geochem. J., 46, 1–9, 2012.

IAEA: Sediment distribution coefficients and concentration factors for biota in the marine environment, Technical Report Series no. 422, IAEA, Vienna, 1–95, 2004.

Inomata, Y., Aoyama, M., and Hirose, K.: Analysis of 50-y record of surface Cs-137 concentrations in the global ocean using the HAM-global database, J. Environ. Monitor. 11 116–125, 2009.

Inoue, M., Kofuji, H., Hamajima, Y., Nagao, S., Yoshida, K., and Yamamoto, M.: ^{134}Cs ^{137}Cs activities in coastal seawater along Northern Sanriku and Tsugaru Strait, northeastern Japan, after Fukushima Dai-ichi Nuclear Power Plant accident, J. Environ. Radioact., 111, 116–119, 2012.

Kaeriyama, H., Watabe, T., and Kusakabe, M.: ^{137}Cs concentration in zooplankton and its relation to taxonomic composition, in the western North Pacific Ocean, J. Environ. Radioact., 99, 1838–1845, 2008.

Kaeriyama, H., Anbe, D., Shigenobu, Y., Fujimoto, K., Ono, T., Tadokoro, K., Okazaki, Y., Narimatsu, Y., and Watanabe, A.: Concentration ratio of radio Cs derived from the Fukushima Dai-ichi nuclear power plant accident for zooplankton in seawater off Fukushima and Miyagi prefectures, Japan, Fall meeting of the Oceanographic Society of Japan, Shimizu, Shizuoka, Japan, 13–17 September 2012, 407, 2012.

Kawamura, H., Kobayashi, T., Furuno, A., Ishikawa, Y., Nakayama, T., Shima, S., and Awaji, T.: Preliminary numerical experiments on oceanic dispersion of ^{131}I and ^{137}Cs discharged into the ocean because of the Fukushima Daiichi Nuclear Power Plant disaster, J. Nucl. Sci. Technol. 48, 1349–1356, 2011.

Kusakabe, M., Ku, T. L., Harada, K., Taguchi, K., and Tsunogai, S.: Chernobyl radioactivity found in mid-water sediment trap interceptor in the N. Pacific and Bering Sea, Geophys. Res. Lett., 15, 44–47, 1988.

Kusakabe, M., Oikawa, S., Takata, H., and Misonoo, J.: Spatiotemporal distributions of Fukushima-derived radionuclides in surface sediments in the waters off Miyagi, Fukushima, and Ibaraki Prefectures, Japan, Biogeosciences Discuss., 10, 4819–4850, doi:10.5194/bgd-10-4819-2013, 2013.

Matsuura, H., Isoda,Y., Kuroda, H., Kuma, K., Saitoh, Y., Kobayashi, N., Aiki, T., Wagawa, T., Yabe, I., and Hoshiba, Y.: Water mass modification process of the passage-flow waters through the Tsugaru Strait. Umi to Sora, 83,21–35 (in Japanese with English abstract), 2007.

MEXT: “Report of Comprehensive Monitoring Plan for radioactivity in the Marine Environments, March 2010” in Japanese.

MEXT: “Report of Comprehensive Monitoring Plan for radioactivity in the Marine Environments, March 2011” in Japanese.

Momoshima, N., Sugihara, S., Ichikawa, R., and Yokoyama, H.: Atmospheric radionuclides transported to Fukuoka, Japan remote from the Fukushima Dai-ichi nuclear power complex following the nuclear accident, J. Environ. Radioact., 111, 28–32 , 2012.

NERH (Nuclear Emergency Response Headquarters), Government of Japan: 2011. Report of Japanese Government to the IAEA Ministerial Conference on Nuclear Safety – The Accident at TEPCO's Fukushima Nuclear Power Stations.

Oikawa, S., Watabe, T., Inatomi, N., Isoyama, N., Misonoo, J., Suzuki, C., Nakahara, M., Nakamura, R., Morizono, S., Fujii, S., Hara, T., and Kido, K.: Plutonium isotopes concentration in seawater and bottom sediment off the coast of Aomori sea area during 1991–2005, J. Environ. Radioact., 102, 302–310, 2011.

Oikawa, S., Watabe, T., Takata, H., Suzuki, C., Nakahara, M., and Misonoo, J.: Progress in the field of marine environmental radioactivity analysis for an offshore fishery monitoring purposes, Bunseki Kagaku (Japanese with English abstract), in press, 2013.

Otosaka, S. and Kobayashi, T.: Sedimentation and remobilization of radiocesium in the coastal area of Ibaraki, 70 km south of the Fukushima Dai-ichi Nuclear Power Plant, Environ. Monitor. Assess., doi:10.1007/s10661-012-2956-7, 2012.

Povinec, P. P., Hirose, K., and Aoyama, M.: Radiostrontium in the western North Pacific: characteristics, behavior and the Fukushima impact, Environ. Sci. Tecnol., 46, 10356–10363, 2012.

Sakai, K. and Hiroe, Y.: Mechanism of nutrient supply to warm-core ring off Sanriku, Japan. J. Oceanogr., 58, 683–690, 2002.

Sakuma, H. and Kawamura, K.: Structure and dynamics of water on Li^+, Na^+, K^+, Cs^+, H_3O^+ exchanged muscovite surfaces: a molecular dynamics study, Geochim. Cosmochim. Acta, 75, 63–81, 2011.

Takata, H., Aono, T., Tagami, K., and Uchida, S.: Sediment–water distribution coefficients of stable elements in four estuarine areas in Japan, Japan, J. Nucl. Sci. Technol., 47, 111–122, 2010.

Tsumune, D., Tsubono, T., Aoyama, M., and Hirose, K.: Distribution of oceanic ^{137}Cs from the Fukushima Dai-ichi Nuclear Power plant simulated numerically by a regional ocean model, J. Environ. Radioact., 111, 100–108, 2012.

UNSCEAR: Sources and Effects of Ionizing Radiation, United Nations Scientific Committee on the Effects of Atomic Radiation. New York, USA, 2000.

Table 1. Sampling stations during the two phases (sampling date: JST).

Station	Latitude (N)	Longitude (E)	Depth (m)* Min.		Max.
23 Mar 2011 to 7 May 2011 (Phase 1)					
1-1	37°40.0′	141°24.0′	125	–	137
1-2	37°35.0′	141°24.0′	131	–	133
1-3	37°30.0′	141°24.0′	134	–	135
1-4	37°23.0′	141°24.0′	140	–	142
2-1	37°16.0′	141°24.0′	148	–	150
2-2	37°12.0′	141°24.0′	150	–	152
2-3	37°06.0′	141°24.0′	171	–	173
2-4	37°00.0′	141°24.0′	182	–	186
2-5	37°00.0′	141°15.0′	146	–	147
2-6	37°00.0′	141°05.0′	101	–	103
1-A	37°45.0′	141°05.0′	25	–	32
1-B	37°42.5′	141°15.0′		61	
S1	37°48.0′	141°05.0′			
S2	37°48.0′	141°15.0′			
S3	36°56.0′	141°19.5′			
S4	36°56.5′	141°05.0′			
9 May 2011 to 21 Feb 2012 (Phase 2)					
1	38°40.0′	142°00.0′	327	–	341
2	38°00.0′	142°00.0′	361	–	373
3	37°20.0′	142°00.0′	691	–	744
4	37°20.0′	142°30.0′	211	–	1210
5	36°40.0′	142°30.0′	3477	–	4379
6	36°40.0′	142°00.0′	2474	–	2492
7	36°00.0′	142°00.0′	3105	–	3430
8	36°00.0′	141°30.0′	1970	–	2215
9	36°40.0′	141°30.0′	798	–	864
10	38°30.0′	143°00.0′		1737	
11	38°30.0′	144°00.0′		7282	
12	38°00.0′	143°00.0′		1854	
13	38°00.0′	144°00.0′		7567	
14	37°30.0′	143°00.0′		3264	

Table 1. Continued.

Station	Latitude (N)	Longitude (E)	Depth (m)*		
			Min.	–	Max.
15	37°30.0′	144°00.0′	6798		
16	37°00.0′	142°00.0′	1360		
17	37°00.0′	143°00.0′	5108		
18	37°00.0′	144°00.0′	6161		
19	36°30.0′	142°00.0′	2755		
20	36°30.0′	143°00.0′	7282		
21	36°30.0′	144°00.0′	5846		
22	36°00.0′	143°00.0′	5971		
23	36°00.0′	144°00.0′	5836		
24	35°30.0′	141°00.0′	120		
25	35°30.0′	142°00.0′	4572		
26	35°30.0′	143°00.0′	6228		
27	35°30.0′	144°00.0′	5761		
A1	38°30.0′	141°51.0′	202	–	212
a1	38°15.0′	141°51.0′	212	–	218
A2	38°30.0′	141°58.0′	302	–	314
A3	38°30.0′	142°05.0′	468	–	498
B1	38°05.0′	141°15.4′	44	–	45
B2	38°05.0′	141°22.4′	74	–	76
B3	38°05.0′	141°29.4′	118	–	122
B4	38°05.0′	141°43.4′	156	–	161
C1	37°45.0′	141°15.4′	55	–	59
C2	37°45.0′	141°22.4′	104	–	109
C3	37°45.0′	141°29.4′	133	–	137
D1	37°35.0′	141°22.4′	123	–	127
D2	37°35.0′	141°29.4′	135	–	138
D3	37°35.0′	141°36.4′	222	–	230
E1	37°25.0′	141°22.4′	132	–	138

Table 1. Continued.

Station	Latitude (N)	Longitude (E)	Depth (m)* Min.	–	Max.
E2	37°25.0′	141°29.4′	153	–	157
E3	37°25.0′	141°36.4′	228	–	243
E4	37°25.0′	141°43.4′	338	–	352
E5	37°30.0′	142°00.0′	531	–	556
F1	37°15.0′	141°22.4′	139	–	146
F2	37°15.0′	141°29.4′	172	–	175
F3	37°15.0′	141°36.4′	230	–	248
G0	37°05.0′	141°08.4′	107	–	110
G1	37°05.0′	141°15.4′	138	–	142
G2	37°05.0′	141°22.4′	161	–	166
G3	37°05.0′	141°29.4′	205	–	216
G4	37°00.0′	141°45.0′	655	–	683
H1	36°55.0′	141°08.4′	130	–	137
H2	36°55.0′	141°15.4′	152	–	158
H3	36°55.0′	141°22.4′	231	–	241
I0	36°45.0′	140°53.0′	72	–	73
I1	36°45.0′	140°57.0′	94	–	101
I2	36°45.0′	141°04.0′	131	–	138
I3	36°45.0′	141°11.0′	181	–	195
J1	36°25.0′	140°43.0′	43	–	50
J2	36°25.0′	140°57.0′	280	–	302
J3	36°25.0′	141°04.1′	530	–	589
K1	36°04.0′	140°43.0′	23	–	33
K2	36°04.0′	140°57.0′	193	–	215
K3	36°04.0′	141°04.0′	470	–	499
L1	35°45.0′	140°57.0′	36	–	45
L2	35°45.0′	141°04.0′	105	–	113
L3	35°45.0′	141°11.0′	140	–	172
L4	35°45.0′	141°18.0′	640	–	850

* Because stations during each cruise were located within 1 nautical mile from a certain point based on a GPS system, depth of each station varied a little. For detailed information on cruise and sampling stations, please see Table 1 in Supplement.

Table 2. Hydrographic parameters, activities, and activity ratios of ^{131}I, ^{134}Cs, and ^{137}Cs in the surface waters during four cruises (i.e., KH11-E01, MR11-E01, KR11-E02, and YK11-E02). For the comparison of the activity ratios of ^{131}I/^{137}Cs and ^{134}Cs/^{137}Cs, samples with no data for ^{131}I were excluded.

Station	Cruise	Sampling date	Depth	Temp.	Salinity	Activity (Bq/L)			Activity ratio	
		(JST)	(m)	(°C)		^{131}I	^{134}Cs*	^{137}Cs*	^{131}I/^{137}Cs	^{134}Cs/^{137}Cs
1-1	KH11-E01	2011/3/23	1	7.5	33.7	24.9 ± 0.6	14.1 ± 0.5	16.4 ± 0.6	1.5 ± 0.1	0.86 ± 0.04
	KH11-E01	2011/3/24	1	7.4	33.7	22.3 ± 0.6	12.9 ± 0.5	15.1 ± 0.6	1.5 ± 0.1	0.85 ± 0.05
	KH11-E01	2011/3/25	1	7.7	33.8	3.5 ± 0.3	–	–		
	KH11-E01	2011/3/26	1	7.8	33.8	18.1 ± 6.1	12.2 ± 4.4	16.4 ± 5.1	1.1 ± 0.5	0.74 ± 0.36
	MR11-E01	2011/4/1	4	7.9	33.7	11.0 ± 3.9	2.0 ± 3.6	4.1 ± 3.8	2.7 ± 2.7	0.48 ± 0.99
1-2	KH11-E01	2011/3/23	1	7.9	33.7	30.0 ± 0.8	11.2 ± 0.6	11.2 ± 0.6	2.7 ± 0.2	1.0 ± 0.1
	KH11-E01	2011/3/24	1	7.5	33.7	16.9 ± 0.6	7.7 ± 0.5	8.3 ± 0.6	2.0 ± 0.2	0.93 ± 0.09
	KH11-E01	2011/3/25	1	7.7	33.8	3.3 ± 0.3	0.7 ± 0.18	0.7 ± 0.2	4.7 ± 1.2	1.1 ± 0.4
	KH11-E01	2011/3/27	1	7.3	33.7	5.4 ± 0.3	1.3 ± 0.2	1.5 ± 0.2	3.6 ± 0.5	0.87 ± 0.19
	MR11-E01	2011/3/30	4	7.8	33.7	3.3 ± 4.4	–	–		
	MR11-E01	2011/4/3	4	7.3	33.7	6.0 ± 3.7	–	–		
1-3	KH11-E01	2011/3/23	1	7.9	33.8	76.8 ± 1.4	21.4 ± 0.9	24.1 ± 1.0	3.2 ± 0.1	0.89 ± 0.05
	KH11-E01	2011/3/24	1	7.7	33.8	57.4 ± 0.9	22.7 ± 0.7	26.1 ± 0.7	2.2 ± 0.1	0.87 ± 0.04
	KH11-E01	2011/3/25	1	7.7	33.8	29.0 ± 0.8	8.7 ± 0.5	8.0 ± 0.5	3.6 ± 0.2	1.1 ± 0.1
	KH11-E01	2011/3/26	1	8.1	33.7	15.3 ± 6.0	1.8 ± 3.5	–		
	MR11-E01	2011/4/1	4	7.7	33.7	2.0 ± 3.6	3.2 ± 3.4	–		
	MR11-E01	2011/4/9	4	8.5	33.5	77.4 ± 4.9	47.6 ± 4.7	44.2 ± 4.8	1.8 ± 0.2	1.1 ± 0.2
1-4	KH11-E01	2011/3/23	1	7.7	33.8	37.3 ± 0.7	16.2 ± 0.6	18.2 ± 0.6	2.0 ± 0.1	0.89 ± 0.04
	KH11-E01	2011/3/24	1	7.8	33.7	59.1 ± 1.0	15.2 ± 0.6	16.0 ± 0.7	3.7 ± 0.2	0.95 ± 0.05
	KH11-E01	2011/3/25	1	7.7	33.7	30.0 ± 0.7	5.4 ± 0.4	5.9 ± 0.4	5.1 ± 0.4	0.92 ± 0.09
	KH11-E01	2011/3/27	1	7.6	33.7	12.0 ± 0.5	3.6 ± 0.3	3.9 ± 0.3	3.1 ± 0.3	0.92 ± 0.12
	MR11-E01	2011/4/3	4	8.0	33.7	11.6 ± 3.9	–	–		
	KR11-E02	2011/4/11	5	9.0	33.5	88.5 ± 5.1	66.5 ± 5.2	71.0 ± 5.7	1.2 ± 0.1	0.94 ± 0.11
	KR11-E02	2011/4/15	4	9.2	33.5	161 ± 6.6	172 ± 8	186 ± 8.4	0.87 ± 0.05	0.92 ± 0.06
2-1	KH11-E01	2011/3/23	1	7.8	33.7	54.7 ± 1.0	12.7 ± 0.6	12.7 ± 0.6	4.3 ± 0.2	1.0 ± 0.1
	KH11-E01	2011/3/24	1	7.9	33.7	40.5 ± 0.9	11.6 ± 0.6	11.1 ± 0.6	3.6 ± 0.2	1.0 ± 0.1
	KH11-E01	2011/3/25	1	7.8	33.7	25.0 ± 0.7	2.8 ± 0.3	3.1 ± 0.3	8.1 ± 0.8	0.90 ± 0.13
	KH11-E01	2011/3/26	1	8.2	33.7	14.0 ± 5.9	16.5 ± 4.4	5.9 ± 4.5	2.4 ± 2.1	2.8 ± 2.2
	MR11-E01	2011/3/28	4	7.9	33.7	7.0 ± 5.0	11.8 ± 4.1	19.6 ± 5.0	0.36 ± 0.27	0.60 ± 0.26
	MR11-E01	2011/4/1	4	8.2	33.7	12.0 ± 4.1	10.2 ± 4.0	15.7 ± 4.4	0.76 ± 0.34	0.65 ± 0.31
	MR11-E01	2011/4/5	3	8.3	33.7	49.7 ± 4.4	41.5 ± 4.2	37.5 ± 4.5	1.3 ± 0.2	1.1 ± 0.2
	MR11-E01	2011/4/9	5	7.9	33.7	8.6 ± 2.6	–	–		
	KR11-E02	2011/4/13	4	8.9	33.6	64.1 ± 4.4	48.0 ± 4.9	54.3 ± 5.2	1.2 ± 0.1	0.88 ± 0.12
	KR11-E02	2011/4/17	4	9.3	33.6	68.4 ± 4.2	88.0 ± 5.9	83.3 ± 6.1	0.82 ± 0.08	1.1 ± 0.1
2-2	KH11-E01	2011/3/23	1	7.6	33.7	42.0 ± 0.9	11.5 ± 0.6	12.8 ± 0.7	3.3 ± 0.2	0.90 ± 0.06
	KH11-E01	2011/3/24	1	8.0	33.7	36.2 ± 0.7	16.3 ± 0.6	16.9 ± 0.6	2.1 ± 0.1	0.96 ± 0.05
	KH11-E01	2011/3/25	1	8.0	33.7	18.0 ± 0.6	2.0 ± 0.3	2.6 ± 0.3	6.9 ± 0.7	0.77 ± 0.13
	KH11-E01	2011/3/27	1	7.7	33.7	15.0 ± 0.5	2.8 ± 0.3	2.3 ± 0.3	6.5 ± 0.8	1.2 ± 0.2
	MR11-E01	2011/3/30	3	8.5	33.7	8.7 ± 4.7	15.8 ± 3.2	8.5 ± 4.5	1.0 ± 0.8	1.9 ± 1.1
	MR11-E01	2011/4/3	4	8.1	33.7	18.3 ± 4.2	7.3 ± 4.3	10.7 ± 4.6	1.7 ± 0.8	0.68 ± 0.50
	MR11-E01	2011/4/7	5	8.4	33.6	56.3 ± 4.3	36.5 ± 3.5	19.8 ± 3.7	2.8 ± 0.6	1.8 ± 0.4
	KR11-E02	2011/4/11	4	8.4	33.6	13.9 ± 3.0	–	–		
	KR11-E02	2011/4/15	4	9.2	33.6	36.6 ± 3.6	41.9 ± 4.5	39.5 ± 4.6	0.93 ± 0.14	1.1 ± 0.2
	KR11-E02	2011/4/19	3	8.9	33.6	18.8 ± 2.9	27.8 ± 3.9	31.6 ± 4.4	0.59 ± 0.12	0.88 ± 0.17
2-3	KH11-E01	2011/3/23	1	7.2	33.7	29.0 ± 0.8	14.7 ± 0.7	15.3 ± 0.7	1.9 ± 0.1	0.96 ± 0.06
	KH11-E01	2011/3/24	1	7.9	33.8	33.4 ± 0.8	12.1 ± 0.5	12.2 ± 0.6	2.7 ± 0.1	0.99 ± 0.07
	KH11-E01	2011/3/25	1	8.8	33.8	13.0 ± 0.5	1.7 ± 0.3	1.7 ± 0.2	7.6 ± 1.1	1.0 ± 0.2
	KH11-E01	2011/3/26	1	8.2	33.8	6.6 ± 5.7	8.2 ± 3.6	2.8 ± 4.2	2.3 ± 4.0	2.9 ± 4.5
	MR11-E01	2011/3/28	4	8.2	33.8	5.7 ± 4.9	1.8 ± 3.4	3.5 ± 4.1	1.6 ± 2.4	0.53 ± 1.17
	MR11-E01	2011/4/1	4	8.6	33.7	8.2 ± 4.0	3.8 ± 3.5	11.7 ± 4.1	0.70 ± 0.42	0.32 ± 0.32
	MR11-E01	2011/4/9	5	8.5	33.7	14.1 ± 3.0	–	–		
	KR11-E02	2011/4/17	4	9.6	33.7	49.0 ± 3.6	52.1 ± 4.8	53.3 ± 5.1	0.92 ± 0.11	0.98 ± 0.13
2-4	KH11-E01	2011/3/23	1	7.3	33.7	39.4 ± 0.8	15.1 ± 0.6	15.2 ± 0.6	2.6 ± 0.1	0.99 ± 0.06
	KH11-E01	2011/3/24	1	7.9	33.7	37.5 ± 0.8	13.3 ± 0.6	13.4 ± 0.6	2.8 ± 0.1	0.99 ± 0.07
	KH11-E01	2011/3/25	1	7.8	33.8	12.0 ± 0.5	2.0 ± 0.3	2.7 ± 0.3	4.4 ± 0.5	0.74 ± 0.12
	KH11-E01	2011/3/27	1	8.4	33.8	8.5 ± 0.4	1.2 ± 0.2	1.6 ± 0.2	5.3 ± 0.8	0.75 ± 0.17
	MR11-E01	2011/3/30	5	8.6	33.8	2.6 ± 4.4	–	–		
	MR11-E01	2011/4/3	4	8.2	33.7	5.6 ± 3.4	3.9 ± 4.2	1.2 ± 4.0	4.8 ± 17	3.4 ± 12
	MR11-E01	2011/4/7	4	8.4	33.7	10.1 ± 2.9	7.9 ± 1.9	9.9 ± 3.0	1.0 ± 0.4	0.80 ± 0.31
	KR11-E02	2011/4/11	4	9.0	33.7	12.6 ± 3.0	–	–		
	KR11-E02	2011/4/15	4	9.5	33.7	34.4 ± 3.6	34.6 ± 4.1	33.3 ± 4.5	1.0 ± 0.2	1.0 ± 0.2
	KR11-E02	2011/4/29	3	9.7	33.4	14.7 ± 2.3	58.0 ± 4.4	53.0 ± 5.3	0.28 ± 0.05	1.1 ± 0.1
2-5	MR11-E01	2011/3/28	3	9.0	33.9	11.8 ± 0.7	3.8 ± 0.5	4.1 ± 0.6	2.9 ± 0.4	0.91 ± 0.18
	MR11-E01	2011/4/1	3	11.3	34.2	7.8 ± 0.6	–	2.0 ± 0.5	3.8 ± 1.1	
	KR11-E02	2011/4/17	4	11.1	33.9	36.6 ± 3.2	38.6 ± 4.5	38.5 ± 4.5	0.95 ± 0.14	1.0 ± 0.2
2-6	MR11-E01	2011/3/30	4	7.7	33.5	79.4 ± 1.0	6.5 ± 0.6	7.2 ± 0.6	11 ± 0.9	0.89 ± 0.11
	MR11-E01	2011/4/3	4	9.4	33.7	37.5 ± 0.7	5.0 ± 0.5	4.8 ± 0.6	7.9 ± 1.0	1.1 ± 0.2
	MR11-E01	2011/4/7	4	9.3	33.8	25.1 ± 3.5	8.8 ± 2.2	–		
	YK11-E02	2011/4/25	5	11.5	33.8	21.5 ± 2.7	38.6 ± 4.3	40.0 ± 4.6	0.54 ± 0.09	0.97 ± 0.16

* Activities of radiocesium below detection are defined as follows: "–" (10 Bq L^{-1} for ^{137}Cs and ^{134}Cs). Samples for direct measurement by gamma-ray spectrometry were 0.5–2 L of water sample in order to provide only radiocesium values. Data on ^{134}Cs and ^{137}Cs at sampling stations where radioiodine was not detected are not shown in this table. Please see Table 1 in Supplement for all the data on radiocesium.

Table 3. Hydrographic parameters, activities, and activity ratios of ^{131}I, ^{134}Cs, and ^{137}Cs in the water below the surface layer (≤ 5 m) during four cruises (i.e., KH11-E01, MR11-E01, KR11-E02, and YK11-E02). For the comparison of the activity ratios of ^{131}I/^{137}Cs and ^{134}Cs/^{137}Cs, samples with no data for ^{131}I were excluded.

Sampling station	Cruise	Sampling date (JST)	Depth (m)	Temp (°C)	Salinity	Activity (Bq/L) ^{131}I	^{134}Cs*	^{137}Cs*	Activity ratio ^{131}I/^{137}Cs	^{134}Cs/^{137}Cs
1-1	KH11-E01	2011/4/1	114	6.7	33.67	2.6 ± 3.5	8.5 ± 3.8	–		
1-2	MR11-E01	2011/3/30	121	6.5	33.64	0.44 ± 4.4	–	–		
1-2	MR11-E01	2011/4/3	120	6.1	33.61	1.6 ± 3.3	–	–		
1-3	MR11-E01	2011/3/28	122	6.6	33.65	0.65 ± 4.7	4.2 ± 3.6	–		
1-3	MR11-E01	2011/4/1	120	6.2	33.62	4.3 ± 3.6	11 ± 4	9.7 ± 4.2	0.44 ± 0.42	1.2 ± 0.7
1-4	MR11-E01	2011/3/30	127	6.0	33.62	2.0 ± 4.3	–	–		
1-4	MR11-E01	2011/4/3	127	6.5	33.65	3.0 ± 3.5	0.48 ± 3.8	1.2 ± 4.0	2.6 ± 9.3	0.41 ± 3.53
2-1	MR11-E01	2011/3/28	137	7.4	33.70	2.2 ± 4.7	3.8 ± 3.7	8.6 ± 4.6	0.25 ± 0.56	0.44 ± 0.48
2-2	MR11-E01	2011/3/30	141	6.3	33.63	0.22 ± 4.3	9.3 ± 2.8	–		
2-4	MR11-E01	2011/4/3	172	5.9	33.60	2.0 ± 3.4	2.1 ± 3.9	3.4 ± 4.2	0.58 ± 1.2	0.63 ± 1.37
2-5	MR11-E01	2011/3/28	132	8.0	33.79	1.9 ± 0.6	–	–		
2-5	MR11-E01	2011/4/1	133	8.0	33.78	4.8 ± 0.5	–	1.9 ± 0.5	2.6 ± 0.8	
2-6	MR11-E01	2011/3/30	83	8.3	33.81	6.1 ± 0.6	2.1 ± 0.5	–		
2-6	YK11-E02	2011/4/25	49	9.6	33.77	22 ± 3	53 ± 5	63 ± 5	0.36 ± 0.05	0.85 ± 0.10

*Activities of radiocesium below detection are defined as follows: "–" (10 Bq L^{-1} for ^{137}Cs and ^{134}Cs) Samples for direct measurement by gamma-ray spectrometry were 0.5–2 L of water sample in order to provide only radiocesium values. Data on ^{134}Cs and ^{137}Cs at sampling stations where radioiodine was not detected are not shown in this table. Please see Table 1 in Supplement for all the data on radiocesium.

Table 4. Hydrographic parameters, activities of ^{90}Sr, ^{134}Cs, and ^{137}Cs, and ^{90}Sr/^{137}Cs activity ratios in the water samples.

Sampling station	Cruise	Sampling date (JST)	Depth (m)	Temperature (°C)	Salinity	Activity (Bq/L)			Activity ratio
						^{90}Sr	^{134}Cs*	^{137}Cs*	^{90}Sr/^{137}Cs
12	KY11-E03R	2011/8/25	3	25.0	33.75	0.0029 ± 0.0005	0.086 ± 0.006	0.11 ± 0.006	0.026 ± 0.004
14	KY11-E03R	2011/8/25	4	25.5	33.82	0.0040 ± 0.0005	0.094 ± 0.006	0.11 ± 0.003	0.036 ± 0.004
20	KY11-E03R	2011/8/26	3	24.9	33.85	0.0037 ± 0.0004	0.087 ± 0.005	0.10 ± 0.003	0.037 ± 0.004
J1	11WM11	2011/9/8	1	22.2	33.06	0.0032 ± 0.0003	0.11 ± 0.01	0.12 ± 0.003	0.027 ± 0.003
J2	11WM11	2011/9/8	1	22.7	32.89	0.0029 ± 0.0003	0.11 ± 0.01	0.13 ± 0.004	0.022 ± 0.002
I1	11WM11	2011/9/9	1	22.5	33.13	0.0022 ± 0.0004	0.084 ± 0.006	0.10 ± 0.005	0.022 ± 0.004
L1	11WM12	2011/10/13	1	20.1	31.47	0.0029 ± 0.0003	0.058 ± 0.003	0.070 ± 0.002	0.041 ± 0.005
K1	11WM12	2011/10/14	1	19.8	32.26	0.0043 ± 0.0004	0.050 ± 0.003	0.063 ± 0.003	0.068 ± 0.008
E5	11WM12	2011/10/19	1	19.8	33.83	0.0025 ± 0.0003	0.056 ± 0.003	0.069 ± 0.002	0.036 ± 0.004
10	KR11-E07R	2011/11/30	7	15.9	34.15	0.0025 ± 0.0004	0.038 ± 0.002	0.048 ± 0.001	0.052 ± 0.008
15	KR11-E07R	2011/12/1	7	16.1	34.04	0.0022 ± 0.0004	0.044 ± 0.002	0.056 ± 0.002	0.039 ± 0.007
I1	11WM13	2011/12/7	1	14.0	33.78	0.0021 ± 0.0004	0.014 ± 0.001	0.020 ± 0.001	0.11 ± 0.02
H1	11WM13	2011/12/7	1	15.4	34.07	0.0017 ± 0.0003	0.019 ± 0.001	0.027 ± 0.001	0.063 ± 0.013
G0	11WM13	2011/12/9	1	13.8	33.73	0.0014 ± 0.0003	0.010 ± 0.001	0.014 ± 0.001	0.10 ± 0.02
G1	11WM13	2011/12/9	1	15.5	34.18	0.0014 ± 0.0003	0.013 ± 0.001	0.019 ± 0.001	0.074 ± 0.017
F1	11WM13	2011/12/9	1	15.2	34.01	0.0017 ± 0.0003	0.015 ± 0.001	0.021 ± 0.001	0.081 ± 0.016
E1	11WM14	2011/12/10	1	13.7	33.70	0.0013 ± 0.0002	0.005 ± 0.0003	0.0069 ± 0.0003	0.19 ± 0.03
E3	11WM14	2011/12/10	1	13.7	33.82	0.0012 ± 0.0002	0.0013 ± 0.0002	0.0029 ± 0.0002	0.41 ± 0.08

[*] Data on ^{134}Cs and ^{137}Cs at sampling stations where radiostrontium was not detected are not shown in this table. Please see Table 1 in Supplement for all the data on radiocesium.

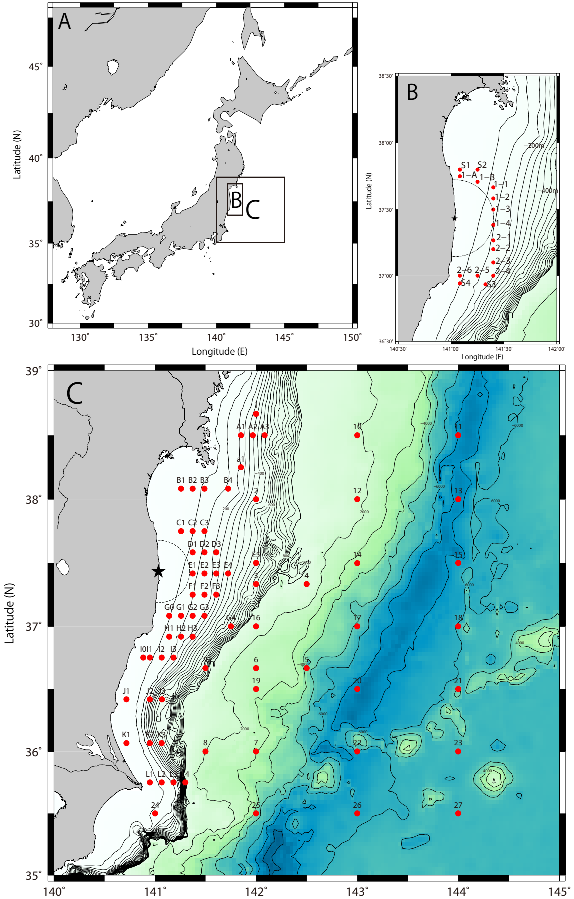

Fig. 1. Locations of sampling areas in coastal areas off Fukushima, Japan **(A)** and sampling stations during Phase 1 (23 Mar 2011 to 7 May 2011) **(B)** and during Phase 2 (9 May 2011 to 21 Feb 2012) **(C)**.

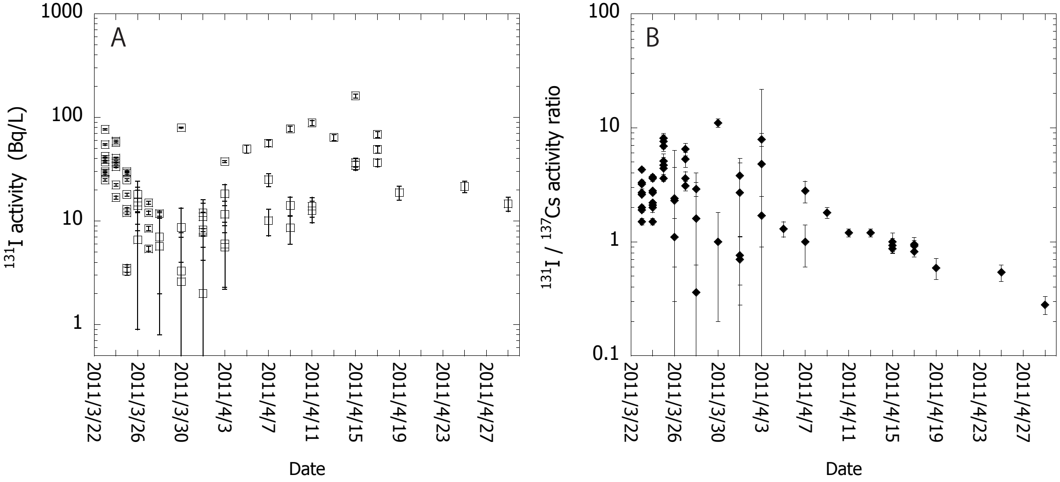

Fig. 2. Temporal changes of ^{131}I activities in surface waters **(A)** and ^{131}I/^{137}Cs activity ratios in surface waters **(B)**. Error bars show one standard deviation based on counting errors by gamma-ray spectrometry.

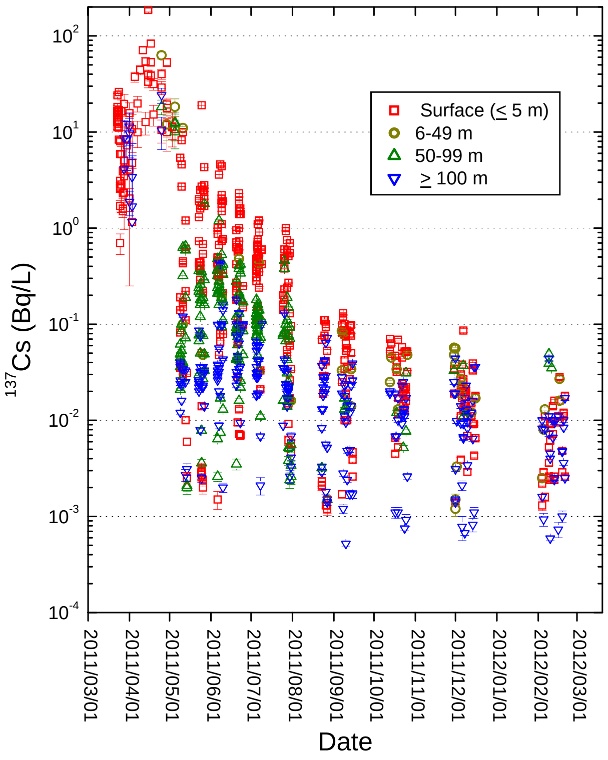

Fig. 3. Temporal variations of ^{137}Cs activities in coastal waters off Miyagi, Fukushima, and Ibaraki from 23 March 2011 to 21 February 2012. Error bars show one standard deviation based on counting errors by gamma-ray spectrometry.

Title Page
Abstract
Introduction
Conclusions
References
Tables
Figures
◀▌ ▐▶
◀ ▶
Back
Close
Full Screen / Esc
Printer-friendly Version
Interactive Discussion

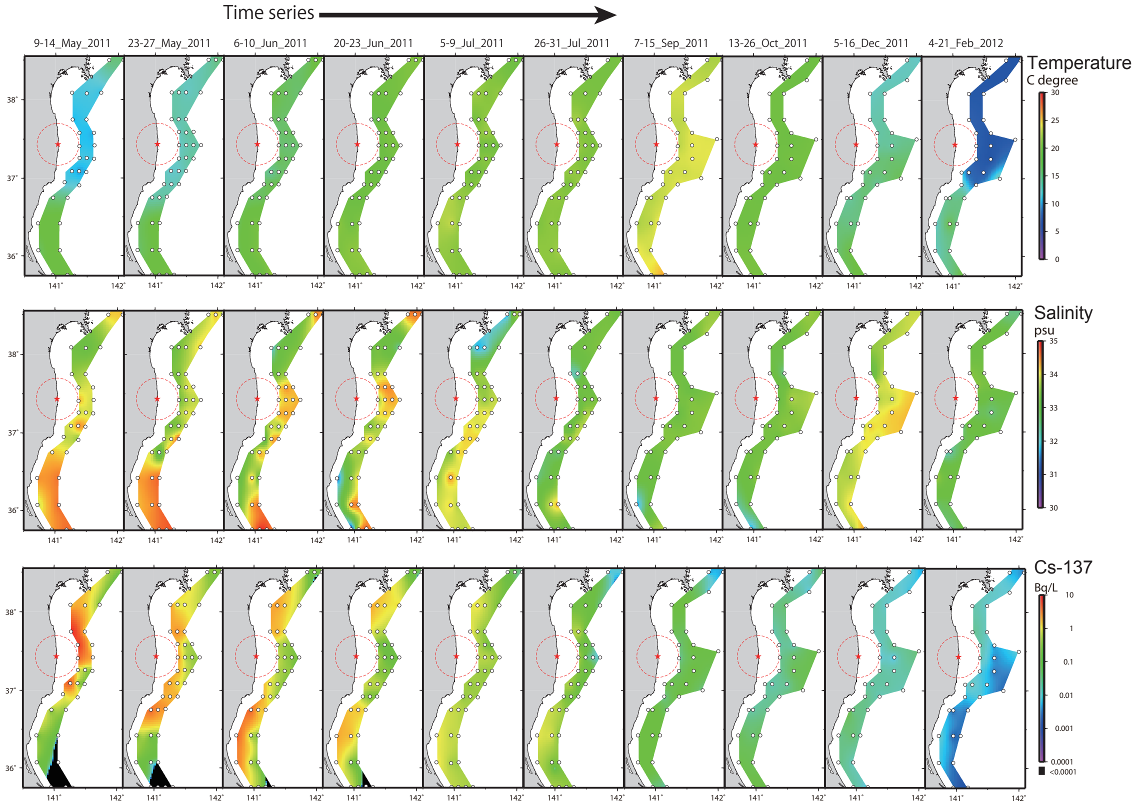

Fig. 4. Distributions of temperature **(A)**, salinity **(B)**, and ^{137}Cs activities **(C)** in surface water from 9–14 May 2011 to 4–21 February 2012.

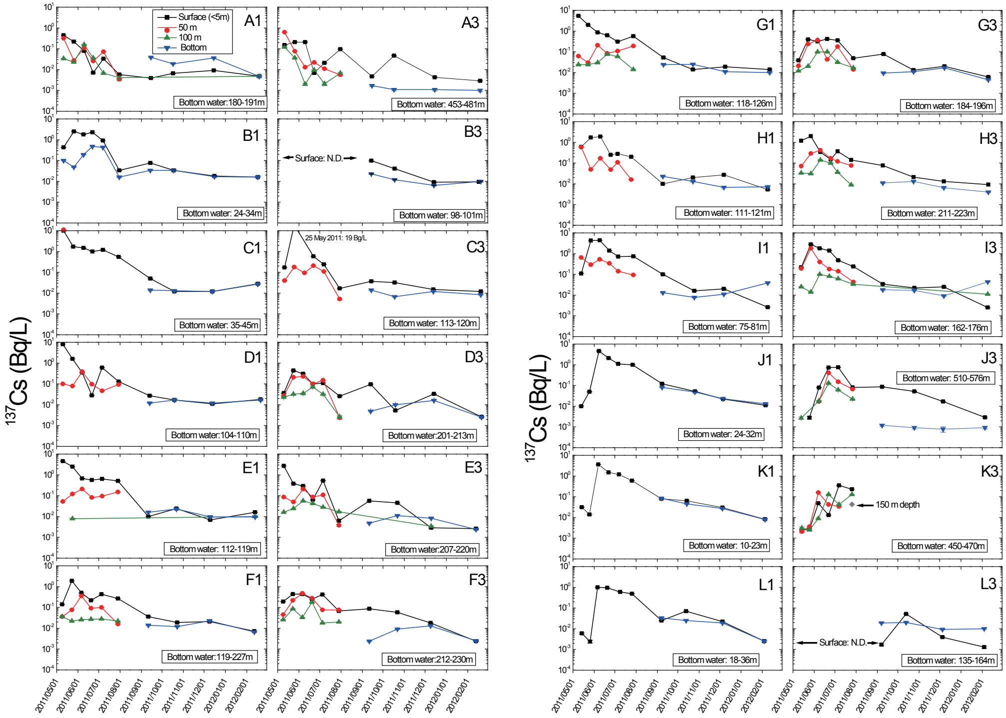

Fig. 5. Temporal variations of ^{137}Cs activities in seawater at each depth. Error bars based on one standard deviation of counting errors are less than or equal to the size of the symbols. Activities of ^{137}Cs in bottom waters at all stations from 9–14 May to 26–31 July were below detection limits.

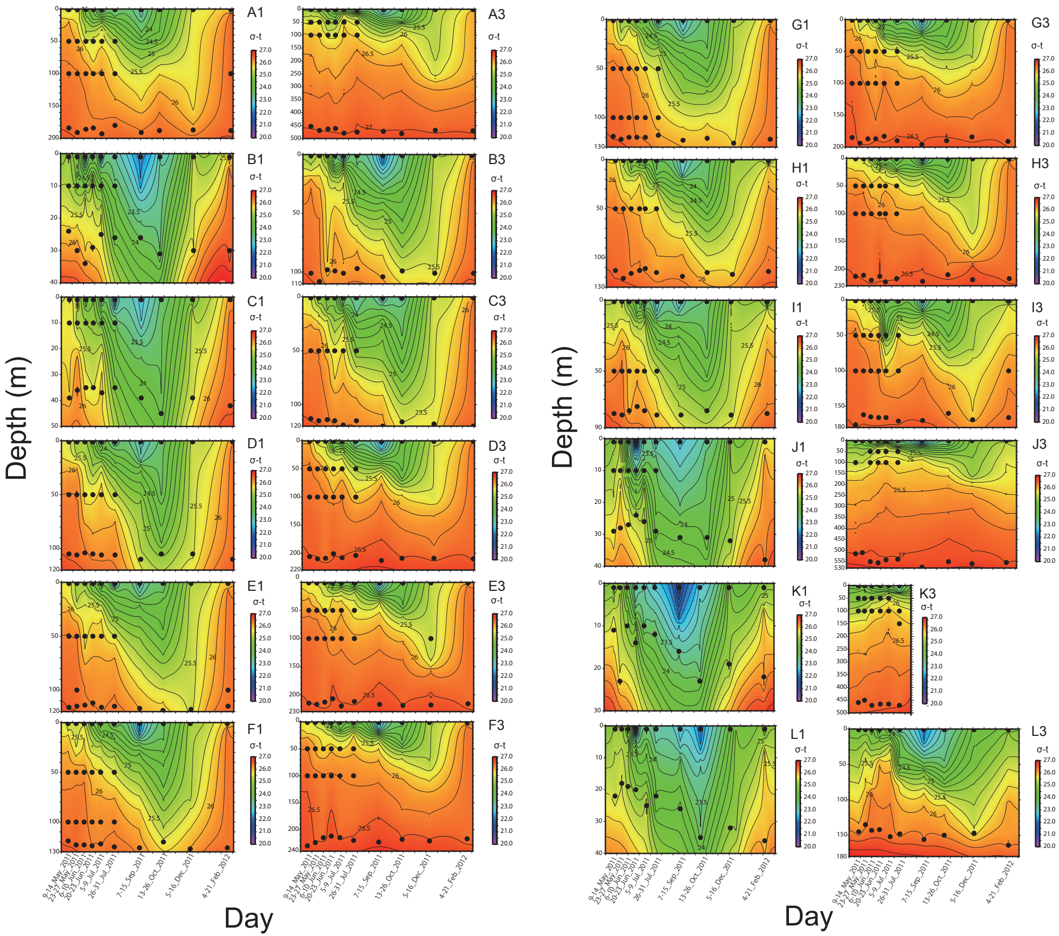

Fig. 6. Vertical sections of σ_t at each station versus time during sampling cruises. Solid circles indicate sampling depths.

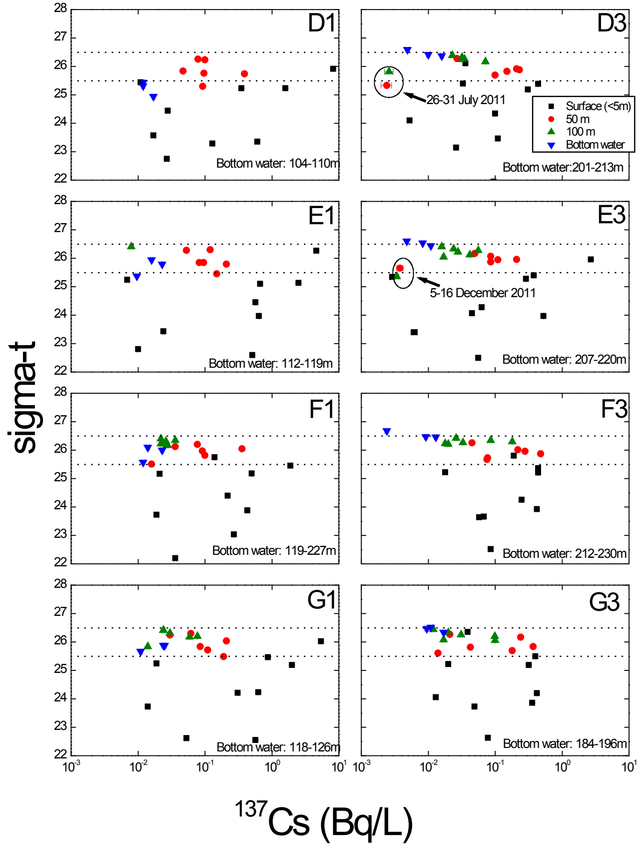

Fig. 7. Activities of ^{137}Cs versus σ_t at each station in coastal waters off Fukushima. Dashed lines indicate the σ_t value range of 25.5–26.5. Error bars based on one standard deviation of counting errors are less than or equal to the size of the symbols.

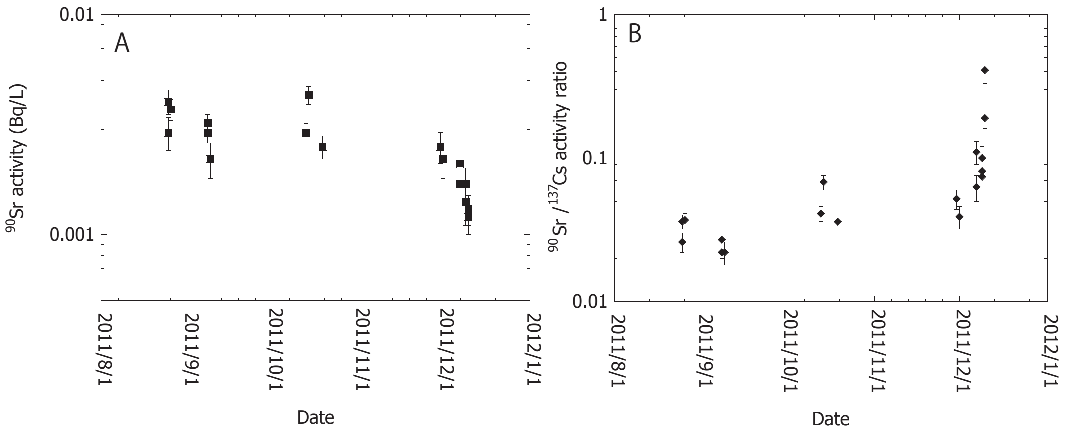

Fig. 8. (A) Temporal change of activities of ^{90}Sr in the surface waters. **(B)** Temporal change of activity ratios of ^{90}Sr to ^{137}Cs in the surface waters.